Investigating distribution patterns of airborne magnetic grains trapped in tree barks in Milan, Italy: insights for pollution mitigation strategies

Journal Article

Author(s):
Vezzola, Laura C.; Muttoni, Giovanni; Merlini, Marco; Rotiroti, Nicola; Pagliardini, Luca; Pelfini, Manuela; Hirt, Ann Marie ⓘD

Investigating distribution patterns of airborne magnetic grains trapped in tree barks in Milan, Italy: insights for pollution mitigation strategies

Laura C. Vezzola,[1] Giovanni Muttoni,[1,2] Marco Merlini,[1] Nicola Rotiroti,[1]
Luca Pagliardini,[1] Ann M. Hirt[3] and Manuela Pelfini[1]

[1]*Dipartimento di Scienze della Terra "A. Desio", Università degli Studi di Milano, via Mangiagalli 34, I-20133 Milano, Italy. E-mail: laura.vezzola@unimi.it*
[2]*ALP—Alpine Laboratory of Paleomagnetism, via Luigi Massa 6, I-12016 Peveragno (CN), Italy*
[3]*Institute of Geophysics, ETH-Zürich, Sonneggstrasse 5, CH-8093 Zürich, Switzerland*

SUMMARY

High levels of air particulate matter (PM) have been positively correlated with respiratory diseases. In this study, we performed a biomonitoring investigation using samples of bark obtained from trees in a selected study area in the city of Milan (northern Italy). Here, we analyse the magnetic and mineralogical properties of the outer and inner barks of 147 trees, finding that magnetite is the prevalent magnetic mineral. The relative concentration of magnetite is estimated in the samples using saturation isothermal remanent magnetization (SIRM) and hysteresis parameters. We also make a first-order estimate of absolute magnetite concentration from the SIRM. The spatial distribution of the measured magnetic parameters is evaluated as a function of the distance to the main sources of magnetic PM in the study area, for example, roads and tram stops. These results are compared with data from a substantially pollution-free control site in the Central Italian Alps. Magnetic susceptibility, SIRM and magnetite concentration are found to be the highest in the outer tree barks for samples that are closest to roads and especially tram stops. In contrast, the inner bark samples are weakly magnetic and are not correlated to the distance from magnetite PM sources. The results illustrate that trees play an important role acting as a sink for airborne PM in urban areas.

Key words: Europe; Environmental magnetism; Rock and mineral magnetism.

1 INTRODUCTION

The metropolitan area of Milan in the Po Valley of northern Italy is plagued by high levels of atmospheric particulate matter (PM) due in part to the 'bowl effect' on atmospheric circulation triggered by the surrounding Alps and Apennines mountain chains (e.g. Masetti *et al.* 2015). Recorded levels of PM with grain size $\leq 10\,\mu m$ (PM_{10}) are often above $100\,\mu g\,m^{-3}$ especially during winter months, with a daily yearly average of $50\,\mu g\,m^{-3}$ (Marcazzan *et al.* 2001; Ozgen *et al.* 2016). It is well known that airborne PM is linked with respiratory illness (Donaldson 2003; Faustini *et al.* 2011; Gualtieri *et al.* 2011; Bigi & Ghermandi 2014; Chiesa *et al.* 2014; Kim *et al.* 2015). Transition metal components such as iron are particularly harmful as they have the potential to produce reactive oxygen species causing inflammation throughout the body (Zhou *et al.* 2003; Birben *et al.* 2012). A recent study by Maher *et al.* (2016) demonstrates that airborne magnetite can enter the brain directly via the olfactory bulb, which can foster Alzheimer disease.

With respect to Milan, Vecchi *et al.* (2008) found high iron PM concentrations, especially during the winter season (average

of $0.0086\,\mu g\,m^{-3}$) compared to the summer season (average of $0.0042\,\mu g\,m^{-3}$). They also found that iron concentration in Milan is higher than in other Italian cities (Florence, Genoa). Iron can come from the abrasion of vehicle brake systems (Hoffmann *et al.* 1999; Sagnotti *et al.* 2006), tram and train rails (Kam *et al.* 2011), as well as from metallurgical processes (Hunt *et al.* 1984). These iron particles bond up with oxygen upon entering the atmosphere to become iron oxides, such as magnetite (Fe_3O_4).

The aim of this study is to monitor airborne iron oxides distribution in a test site in Milan. We selected a municipal park surrounded by tram lines/stops and roads characterized by intense daily traffic, which represent obvious sources of iron PM, among other types of pollutants. We opted to sample tree barks as natural repositories (sinks) of these iron PM sources, and to study them with standard rock-magnetic techniques to define type and concentration of ferro(i)magnetic iron oxide minerals contained therein. Tree barks are preferred to the more frequently used tree leaves (e.g. Matzka & Maher 1999; Hanesch *et al.* 2003; Moreno *et al.* 2003; Lehndorff *et al.* 2006; McIntosh *et al.* 2007; Maher *et al.* 2008; Szönyi *et al.* 2008), because they accumulate airborne PM the entire year. This
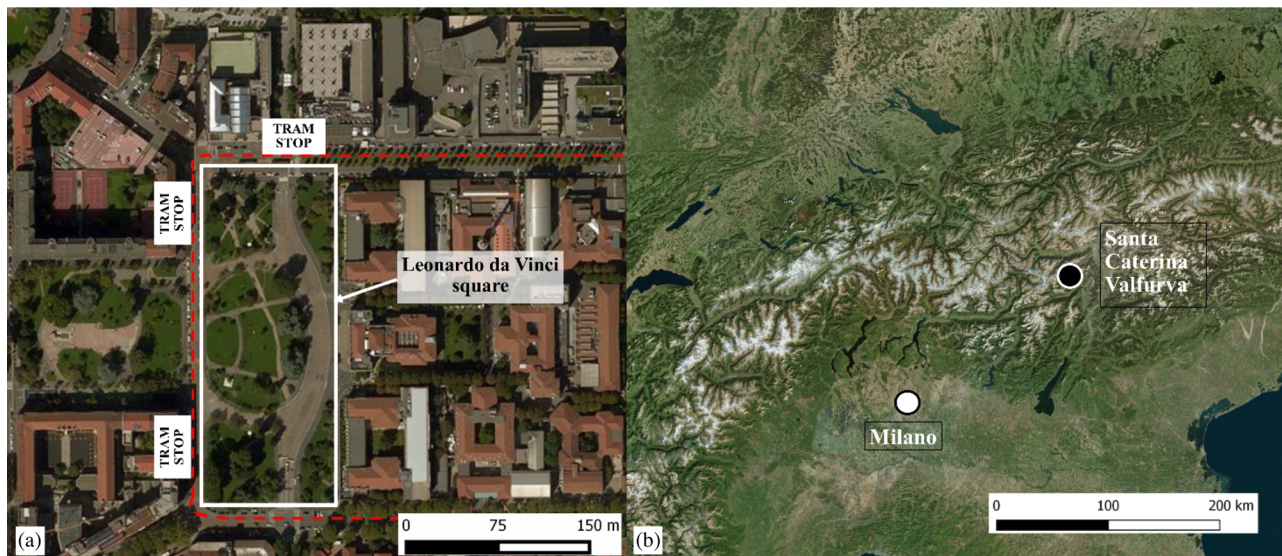
Figure 1. (a) Leonardo da Vinci square in Milan with the closest tram stops. The red discontinuous lines represent the closest roads. (b) Location map of the study area including Milan and Santa Caterina Valfurva.

is important because PM pollution levels are highest in the winter, when leaves of deciduous species, which are dominant in Milan, are absent. Tree bark is already considered as a valuable indicator for monitoring air quality, for instance by applying Instrumental Neutron Activation Analysis (INAA) and Radionuclide X-Ray Fluorescence Analysis (RXRFA) techniques (e.g. Bohm *et al.* 1998; Pacheco *et al.* 2001), and measurements of trace element concentration (e.g. Sawidis *et al.* 2011; Guéguen *et al.* 2012). However, until now only a very limited number of studies have investigated the potential of measuring magnetic parameters of tree bark for monitoring air pollution (Flanders 1994; Kletetschka *et al.* 2003; Zhang *et al.* 2008; Kletetschka 2011). We are not aware of any previous biomonitoring studies conducted in this city, so we present the first results obtained through this approach for the selected study area. The ultimate goal of this study is to quantify on a map the areal dispersion of iron oxides from their sources (e.g. tram stops) to their sinks (tree barks). This could help designing pollution shielding solutions using non-deep tree belts or synthetic bark panels placed at optimal distance and orientation relative to pollution sources.

2 MATERIALS AND METHODS

2.1 Study area

This study was conducted in the 25 000 m^2 municipal park of Leonardo da Vinci Square (Fig. 1a), located in the eastern part of Milan, at an altitude of about 120 m a.s.l. (centre latitude: 45.478096°N; longitude: 9.22569°E). The area is characterized by intense daily traffic; on a typical working day, the number of cars passing through the study area ranges between 6000 and 7000 (Municipality of Milan, Agenzia Mobilità Ambiente Territorio), and trams circulate with a frequency of one every 3–8 min. For the purpose of this study, the area was divided in two portions: an external belt named Area 1, about 20 m wide and located close to the surrounding roads and tram lines/stops, and a more internal Area 2 extending more than 20 m away from the roads (Fig. 1a).

The results obtained in Milan are compared with data from a low-pollution control site. Sampling at the control site was conducted in the village of Santa Caterina Valfurva (hereafter Santa Caterina),

Table 1. List of species and the number of trees sampled for each species at the Milan test site.

Tree species	Number of sampled trees	Tree species	Number of sampled trees
Abies alba	2	*Ilex aquifolium*	11
Acer negundo	5	*Pinus nigra*	4
Acer saccharinum	4	*Populus alba*	2
Catalpa bignonioides	9	*Populus nigra*	11
Cedrus atlantica	16	*Prunus laurocerasus*	4
Cercis siliquastrum	3	*Prunus padus*	32
Cupressus arizonica	4	*Sophora japonica*	21
Cupressus glabra	2	*Taxus baccata*	2
Fagus sylvatica	2	*Tilia cordata*	13

belonging to the municipality of Valfurva, characterized by 2600 inhabitants, with very reduced car traffic and absence of trains and trams. The village is located 200 km north of Milan, in Valtellina (central Alps) at an elevation of about 1700 m a.s.l. (Fig. 1b), in a typical Alpine environment shaped by glaciers and mass wasting processes (e.g. Del Ventisette *et al.* 2012; Pelfini *et al.* 2014).

2.2 Sampling

Sampling in Milan was conducted on the 2014 November 22, 24 and 25 on trees belonging to 18 different species including, among others, *Prunus padus*, *Sophora japonica* and *Cedrus atlantica* (see Table 1 for a complete list). Sampling at the test site in Santa Caterina was conducted on 2015 July 27 on trees of *Picea abies* species. At both localities, the selected tree species show similar bark textures: fissured, rugose and coarse-grained (Fig. 2). The absorption properties of these fractal surfaces on airborne micrometric particles are considered analogous, irrespective of taxonomic attribution.

A total of 147 trees were sampled in the Milan test site and 20 trees in the Santa Caterina control site. The position of each tree was recorded using Global Positioning System. Each sample consisted of a cylindrical fragment of trunk bark, extracted at approximately 1.5 m above the ground from the tree-side exposed in the direction of the closest street, using a steel extractor tool with a diameter of 2.5 cm. The bark samples were placed in 10 cm^3 plastic boxes and
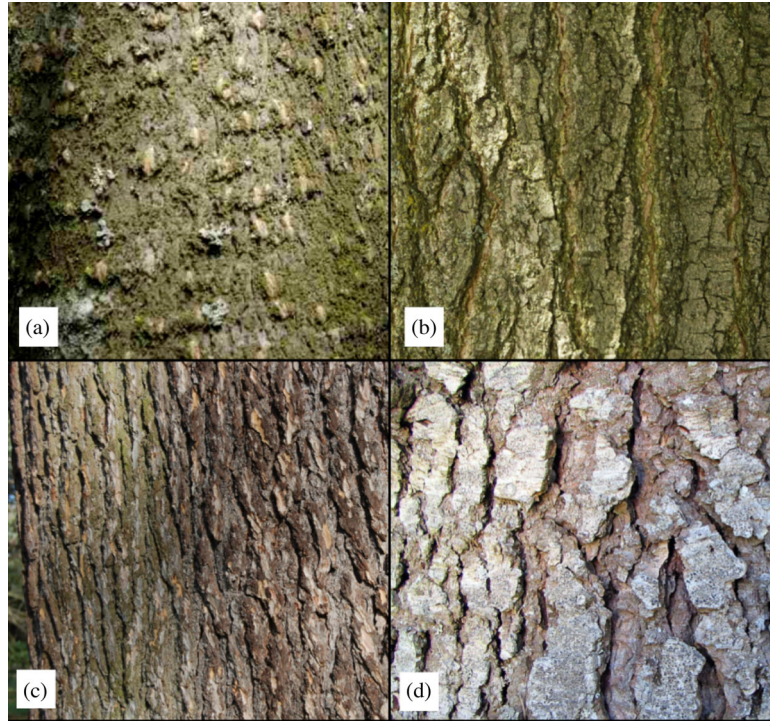
Figure 2. Tree bark texture of (a) *Prunus padus*, (b) *Sophora japonica*, (c) *Cedrus atlantica* and (d) *Picea abies*.
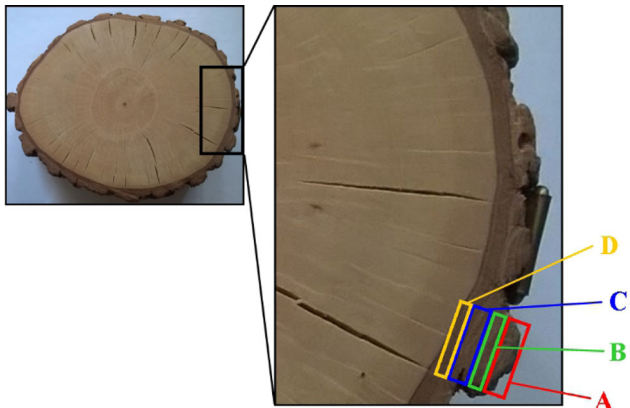

Figure 3. Explanatory image showing the position of tree bark samples from outer to inner bark, labelled 'A', 'B', 'C' and 'D'.

closed with plastic tops. For the Milan test site, a total of 99 out of 147 bark samples were cut in the laboratory, using a ceramic knife that we cleaned with ethanol after cutting each sample, into an outer disc sample (i.e. at the contact with the atmosphere) and an inner disc sample, which were labelled 'A' and 'B', respectively. In 48 particularly thick samples, up to a maximum of four disc samples were obtained ('A', 'B', 'C' and 'D' arranged from the outside to the inside; Fig. 3). The remaining 35 samples yielded only an outer 'A' sample, that is, subsampling was not possible. In total, 278 samples of trunk bark were obtained from the Milan test site. With regards to the control site of Santa Caterina, we extracted one sample of outer bark from each tree for a total of 20 'A' bark samples. All samples were weighed in order to normalize the measurements by sample mass and then refrigerated at 5 °C until the day before the analyses. Normalization was based on weight because all the samples have very similar surface areas (5 cm^2), hence normalization based on surface area would not alter the areal distribution of values.
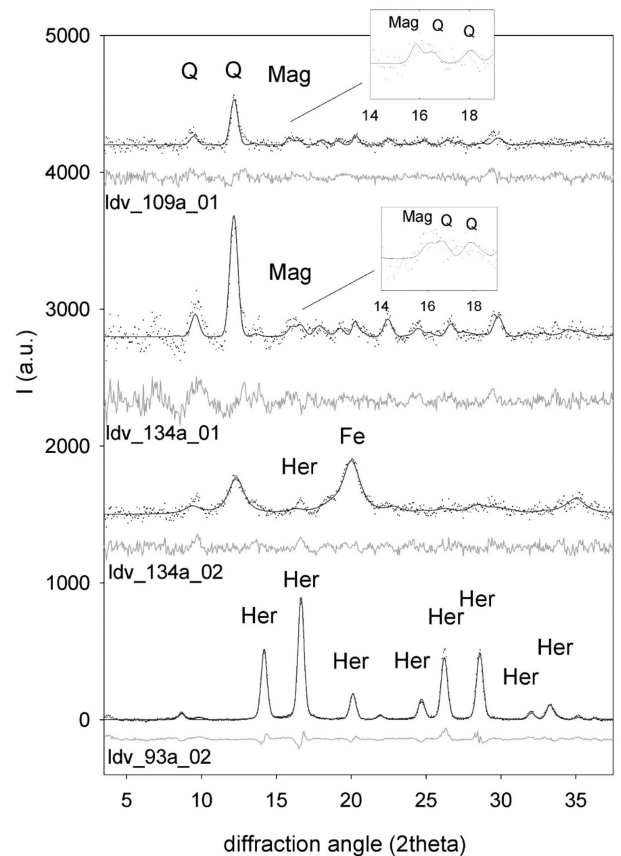

Figure 4. Experimental laboratory X-ray powder microdiffraction pattern (dotted), fitted (line) and difference curve computed by Rietveld fit of selected fragments. The samples are labelled in the figure. The main diffraction peaks are indicated: quartz, SiO_2 (Q), metallic iron (Fe), hercynite, $FeAl_2O_4$ (Her) and magnetite, Fe_3O_4 (Mag).
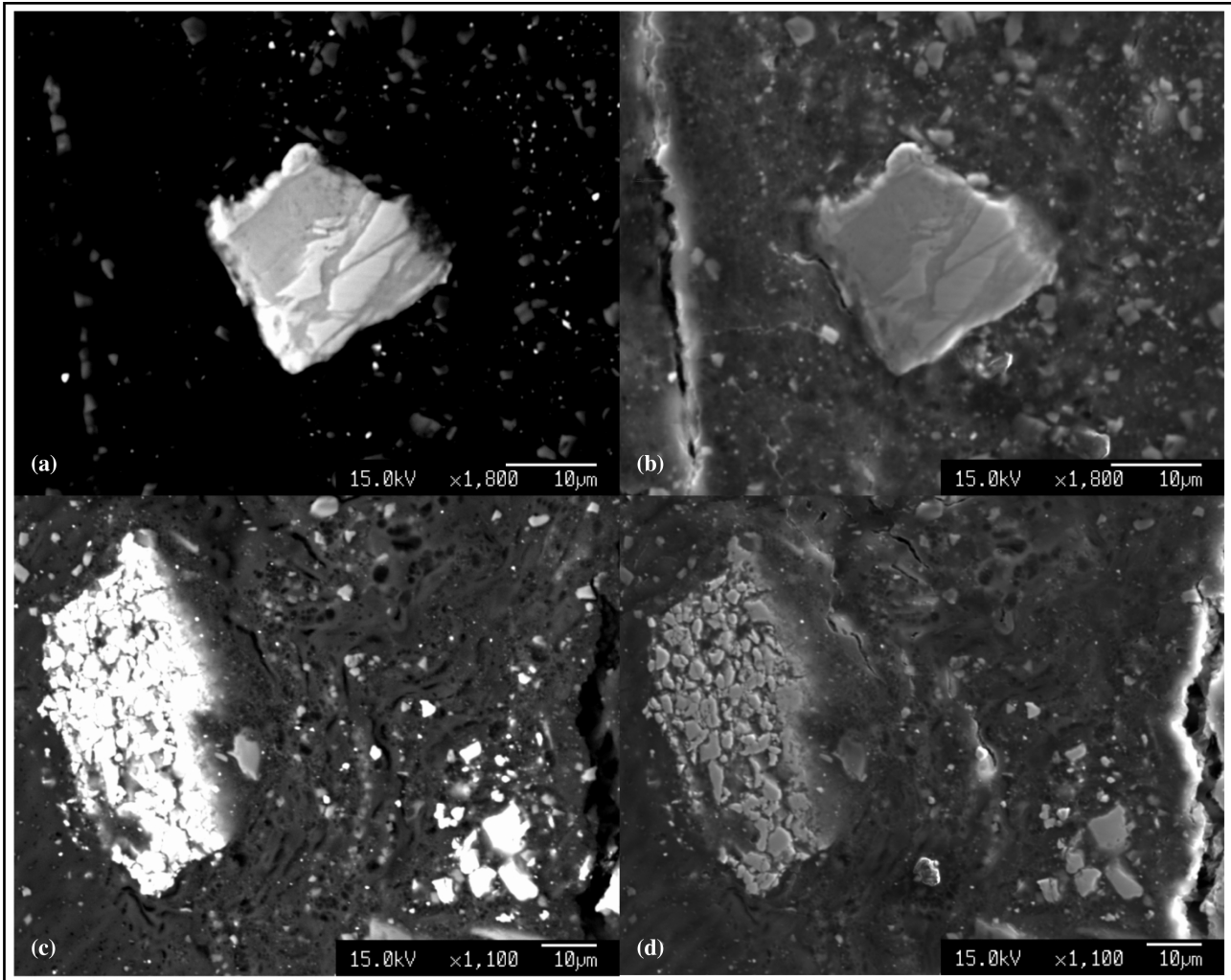
Figure 5. (a) and (c) Angular iron oxide particles found in 'A' bark sample (outer bark) analysed at the microprobe and (b) and (d) secondary ion image showing the integration of the particle in the 'A' bark sample. The X-ray and rock-magnetic analyses showed that it consists of magnetite.
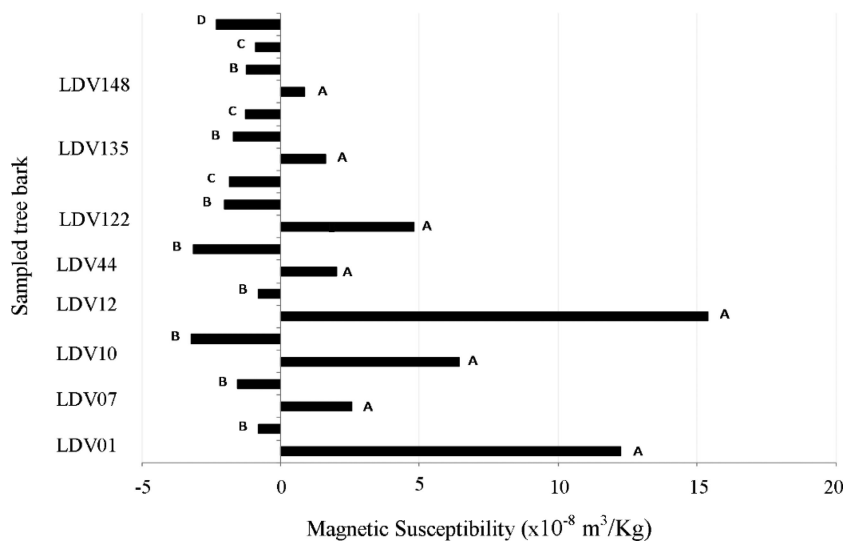

Figure 6. Mass-specific magnetic susceptibility values on representative samples of tree bark. In the reported examples, outer bark (named 'A') always shows higher and positive susceptibility values than the inner bark (named 'B', 'C' and 'D').

Table 2. Average values of magnetic susceptibility and SIRM measured on the analysed samples. For bark layers A and B, we distinguished between Area 1 (closer to the roads, i.e. <20 m) and Area 2 (farer from the roads, i.e. >20 m).

Measured parameter	Bark layer	Area	Average ± SD	Number of samples
Magnetic susceptibility ($\times 10^{-8}$ m^3 Kg^{-1}) Milan	A	1	1.25 ± 4.2	60
		2	0.52 ± 3.5	87
	B	1	−1.31 ± 1.9	38
		2	−2.26 ± 2.8	65
	C		−1.32 ± 1.7	16
	D		−1.76 ± 0.7	3
Magnetic susceptibility ($\times 10^{-8}$ m^3 Kg^{-1}) Santa Caterina	A		−9.87 ± 0.59	20
SIRM ($\times 10^{-6}$ Am^2 Kg^{-1}) Milan	A	1	15.53 ± 18.5	42
	B	2	9.88 ± 10.2	40
	C	1	2.23 ± 2.5	42
	D	2	2.06 ± 3.4	25
			1.56 ± 2.1	10
			0.45 ± 0.2	2
SIRM ($\times 10^{-6}$ Am^2 Kg^{-1}) Santa Caterina	A		0.21 ± 0.16	20

2.3 Mineralogical analyses

The mineralogy of three 'A' bark and two 'B' bark samples from Milan was investigated by X-ray diffraction (XRD) and electron microprobe analysis. X-ray microdiffraction was performed in transmission geometry on aggregates of mineral particles with 30–150 μm size, extracted directly from the tree bark. Measurements were made on an Oxford X'Calibur instrument with Mo X-ray source ($\lambda = 0.710$ Å), polycapillary focusing optics (beam size on the sample approximate 150 μm) and CCD detector. The 2-D diffraction data were integrated with the CrysalisRed software and the identification of mineral phases was first achieved by comparison with PDF-2 database, followed by Rietveld refinement. Chemical analysis was performed with an electron microprobe (JEOL JXA 8200), equipped with Wavelength Dispersive X-Ray Spectrometers (WDSs).

2.4 Magnetic analyses

The initial magnetic susceptibility of all samples was measured using an AGICO KLY-2 Kappabridge. A subset of 181 samples was then magnetized at room temperature in incremental fields up to 1 T or occasionally 2.5 T using an ASC Pulse Magnetizer. The resulting isothermal remanent magnetization (IRM) was measured after each step on a 2G Enterprises DC SQUID cryogenic magnetometer located in a magnetically shielded room. Mass-specific susceptibility and saturation IRM (SIRM) values were calculated. The *S*-ratio was calculated as IRM$_{300\,\text{mT}}$/SIRM (Evans & Heller 2003), where IRM$_{300\,\text{mT}}$ is the IRM induced in a field of 0.3 T and the SIRM is the IRM at 2.5 T. Hysteresis loops were measured on a subset of 16 representative 'A' bark samples from the Milan test site, using a Micromag 2900 Alternating Gradient Magnetometer, on samples whose saturation IRM was $>5 \times 10^{-6}$ Am^2 Kg^{-1}. The obtained hysteresis loops were corrected for high field susceptibility to obtain the saturation magnetization (M_s) and saturation remanent magnetization (M_{rs}). Measurements were made at the Alpine Laboratory of Palaeomagnetism of Pevergno (Italy) and at the Laboratory of Natural Magnetism of ETH-Zürich (Switzerland).

2.5 Data mapping

Magnetic susceptibility and SIRM values from the Milan test site were plotted in geographic information system (GIS) environment in order to map their areal distribution and distance relative to the surrounding roads and tram lines/stops. Since the sampled trees are relatively evenly distributed in the Milan test site, inverse distance weighted (IDW) interpolation was applied (Johnston *et al.* 2001).

3 RESULTS

3.1 Mineralogical analyses

The XRD analysis indicates that the most common mineral phase in the analysed 'A' bark samples is quartz. However, 'A' bark samples with high susceptibility also contain magnetite (Fe$_3$O$_4$) and/or iron, and only XRD can detect them in weaker magnetic samples. In one sample, a fragment with metallic lustre was identified as hercynite (FeAl$_2$O$_4$), as shown by the powder patterns fitted with Rietveld method (Fig. 4).

The analysis on the electron microprobe on 'A' bark samples confirms the presence of an iron oxide phase interpreted as magnetite with grain size of about 20 μm (Fig. 5a). Secondary ion images reveal that some of the magnetite particles are well inserted in the 'A' bark samples, and not just deposited on their external surface (Figs 5b and d). Moreover, some of the magnetite grains appear have undergone reductive dissolution (Figs 5c and d).

3.2 Magnetic analyses

Samples from the Milan test site show a clear trend in the magnitude of magnetic susceptibility, which was found to strongly decrease from the outer 'A' bark samples to the inner ('B', 'C' and 'D') samples in the same tree (see Fig. 6 and Table 2). The majority of the inner 'B', 'C' and 'D' samples are diamagnetic, which indicates that the organic matter signal dominates the susceptibility. No trend is instead detected within the various inner bark samples, that is, the susceptibility of the 'B' samples is not higher than the 'C' or the 'D' samples. The outer 'A' bark samples from the control site at Santa Caterina show very low values of magnetic susceptibility, comparable to values found in inner 'B' bark samples at the Milan test site (Table 2).

Backfield remagnetization of SIRM of representative 'A' bark samples from Milan and Santa Caterina show the presence of a low coercivity magnetic phase that saturates in fields of ∼200 mT, which is compatible with magnetite that was identified by XRD (Fig. 7). A decrease in the magnitude of the saturation IRM (SIRM)
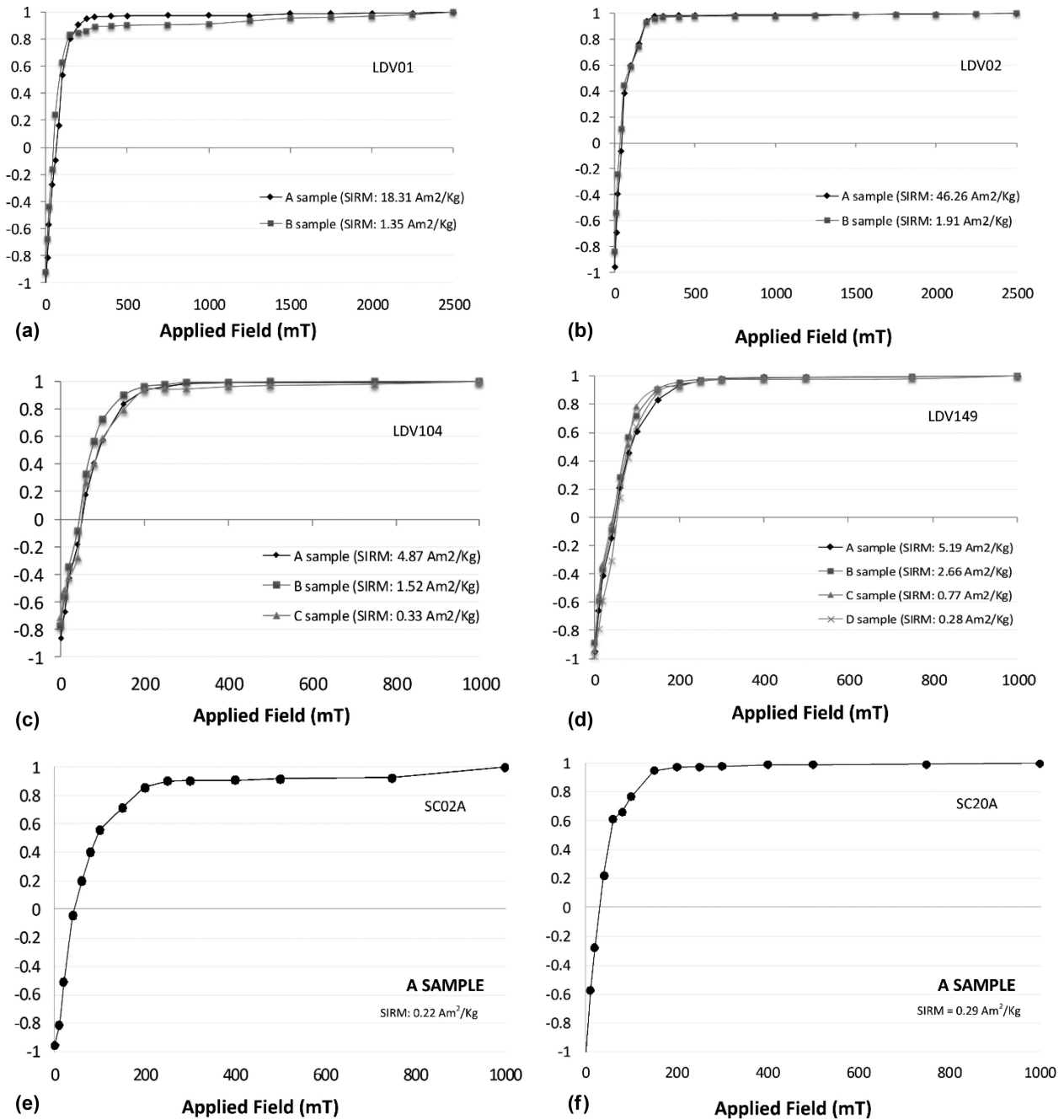
Figure 7. Normalized mass-specific backfield remagnetization of SIRM on representative bark samples from the Milan test site (panels from a to d), showing the presence of variable amounts of a low coercivity magnetic component interpreted as magnetite. Outer 'A' bark samples have always higher values (higher magnetite concentration) than inner 'B' or 'C' or 'D' bark samples. Panels (e) and (f) represents backfield remagnetization of SIRM from two 'A' samples from the control site at Santa Caterina.

from the outer 'A' bark samples to the inner ('B', 'C' and 'D') bark samples is observed (Fig. 7a–d; Table 2). The *S*-ratios show values approaching 1 with no differences detectable between 'A' and 'B' samples, confirming the presence of the low coercivity mineral, magnetite. The outer 'A' samples from the control site at Santa Caterina have SIRM magnitudes that are much lower than the 'A' samples from the Milan test site (Fig. 7e and f; and Table 2).

The magnetic susceptibility and saturation IRM values of 'A' samples from the various tree species sampled at the Milan site show a high degree of variability and high standard deviations (Figs 8a and b). No statistical tests could be performed due to the very

different number of samples available for each species, however, no clear intraspecific trends were observed as well. We stress that the dynamics of passive accumulation of micrometric airborne particles on an absorbing surface (bark) is controlled primarily by physical factors, such as air turbulence, moisture, etc., provided the absorbing surfaces are characterized by similar macroscale rugosity and textures irrespective of their taxonomic attributions.

With regards to the hysteresis analyses, most of the 16 'A' samples from Milan showed an open loop with a varying contribution from the high-field paramagnetic components (Figs 9a–c). These features reflect the presence of a low coercivity ferrimagnetic
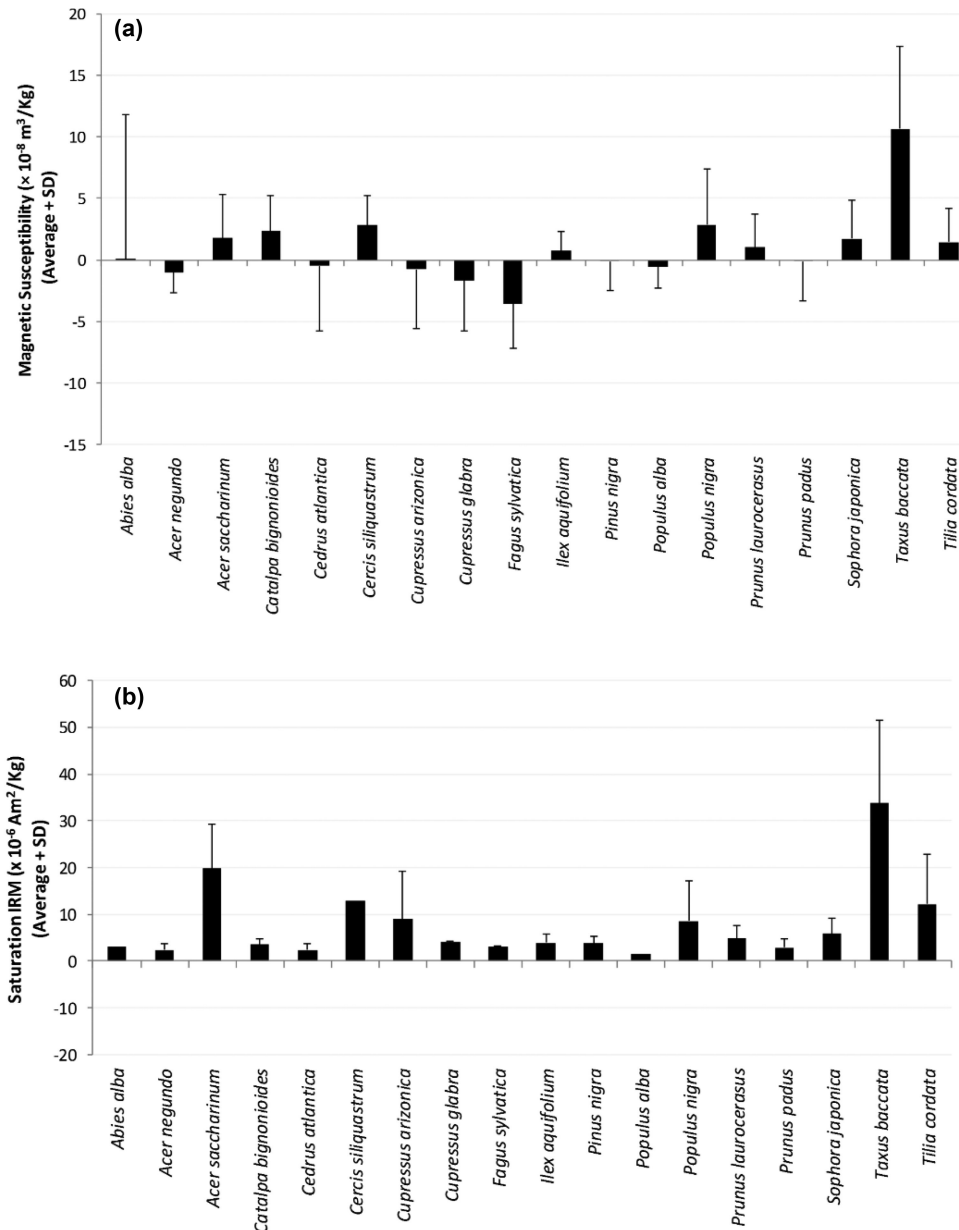
Figure 8. (a) Magnetic susceptibility and (b) saturation IRM for the sampled 'A' tree species at the Milan site. High variability and SD can be observed for both parameters. In the case of saturation IRM, some tree species do not show the SD value due to the analysis of only one sample for that species.

mineral coexisting with a paramagnetic (positive slope) contribution. Some samples, however, show only a paramagnetic magnetization, due to non-ferrimagnetic material, that is, bark (e.g. Fig. 9d). The M_{rs}/M_s ratios range between 0.07 and 0.14 (mean of 0.09, standard deviation of 0.02), which is compatible with pseudo-single domain to multidomain magnetite (Dunlop 2002). This agrees with microprobe observation.

3.3 Mapping of magnetic grains distribution

Distribution maps of magnetic susceptibility and SIRM values for the Milan test site are shown in Figs 10 and 11. The sample locality is subdivided into Area 1, which is within 20 m of the roads and Area 2 with is >20 m from the roads. The map of magnetic susceptibility for 'A' bark samples (Fig. 10a) shows higher mean values in

Area 1 compared to Area 2, with the highest values near tram stops. The low susceptibilities in Area B are comparable to those observed at the control site in Santa Caterina (SC on scale bar in Fig. 10a). The spatial distribution of susceptibility of the inner 'B' samples shows little variability: there is no notable difference between Areas 1 and 2, although the 'B' samples with highest susceptibility are found at the same location where the 'A' sample has high susceptibility (Fig. 10b).

A similar pattern is also found in the spatial distribution of the SIRM, which shows higher mean values for 'A' samples in Area 1, especially near tram stops, while 'A' samples from Area 2 display lower values, which are comparable to the control site in Santa Caterina (Fig. 11a). Inner 'B' samples from both Areas 1 and 2 display low SIRM values and no relationship with distance from tram lines/stops (Fig. 11b).
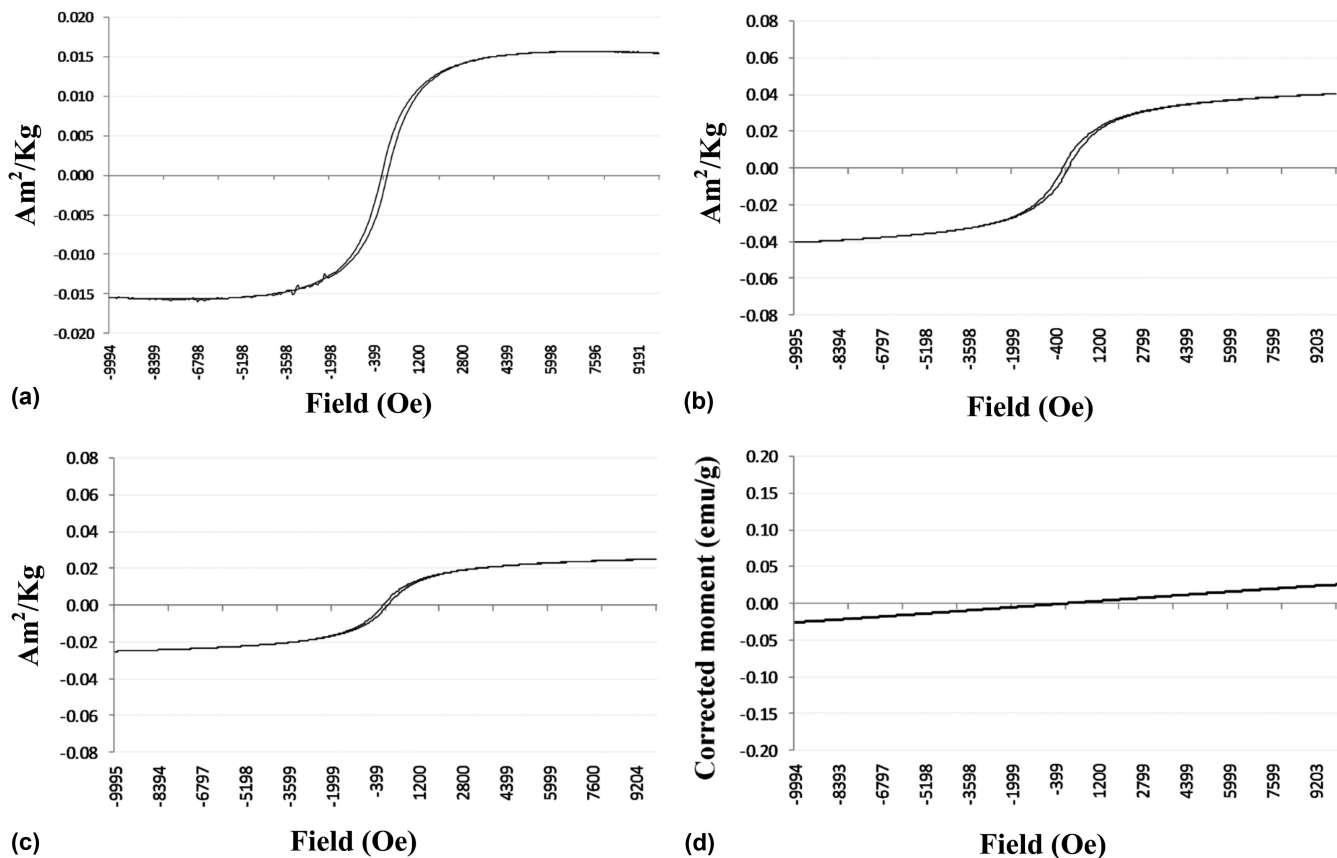
Figure 9. Hysteresis loops on four representative samples. (a)–(c) Most of the analysed samples show hysteresis and (d) is an example of sample that only displays paramagnetic mineralogy.
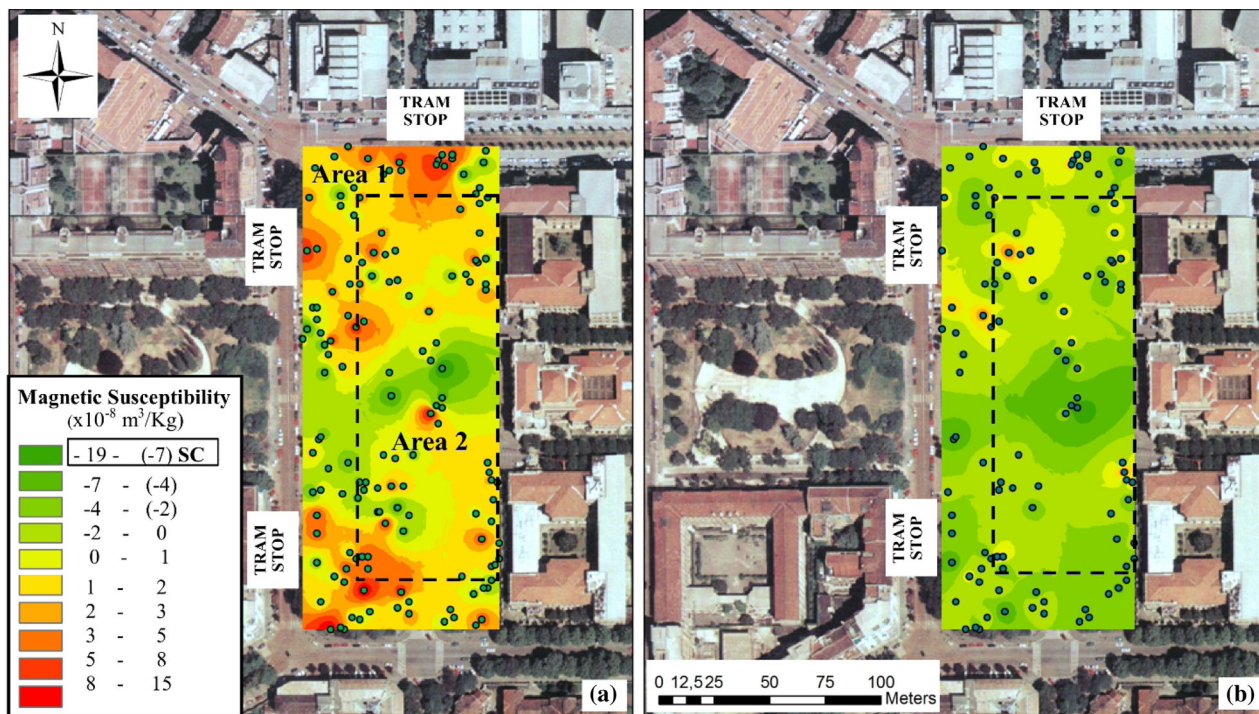

Figure 10. Spatial distribution (defined using inverse distance weighted interpolation in GIS environment) of the magnetic susceptibility values of outer 'A' bark samples (panel a to the left) and inner 'B' bark samples (panel b to the right) recorded at the test site in Milan. The highest values are recorded in 'A' bark samples obtained from trees in Area 1, closer to the roads (distance ≤20 m) and, in particular, closer to the tram stops. Samples from the control site at Santa Caterina (SC on colour scale in panel a) are characterized by low values, belonging to the lowest category detected in the study area in Milan.

Figure 11. Spatial distribution (defined using IDW interpolation in GIS environment) of the saturation IRM (SIRM) values in outer 'A' bark samples (panel a to the left) and inner 'B' bark samples (panel b to the right) recorded at the test site in Milan. The highest values are recorded in 'A' bark samples in Area 1, closer to the roads and tram stops (distance ≤20 m). Samples from the control site at Santa Caterina (SC on colour scale in panel a) are characterized by values belonging to the lowest category detected in the study area in Milan.

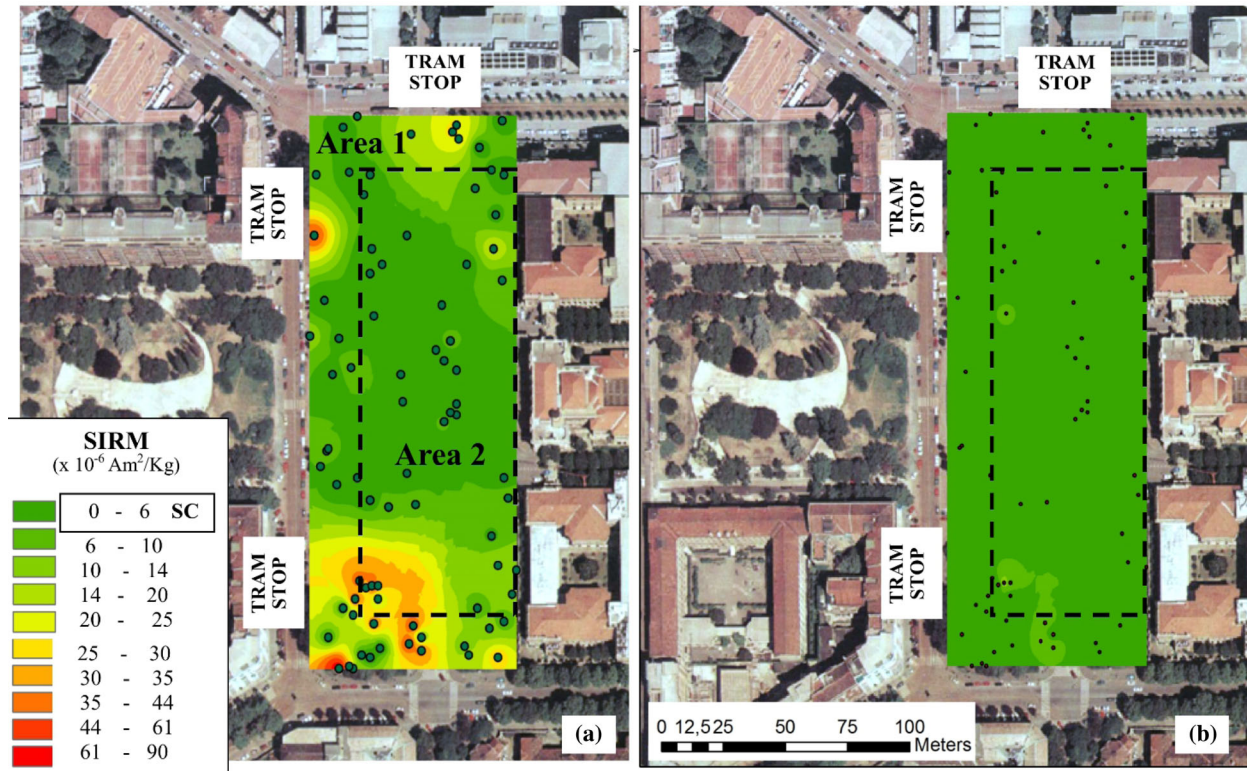A positive linear relationship between magnetic susceptibility and SIRM was obtained for 'A' samples in Area 1 ($R^2 = 0.89$; $p = 2.4 \times 10^{-4}$; Fig. 12a). A similar positive linear relationship exists also for 'A' samples from Area 2, but at a lower statistical level ($R^2 = 0.18$; $p = 3.8 \times 10^{-5}$; Fig. 12a). No statistical correlation is found for the 'B' samples in both Areas 1 and 2 (Fig. 12b). A positive relationship between susceptibility and SIRM can indicate variation in the volume fraction of the ferro(i)magnetic phase(s), and this variation could be caused by a higher number of particles with same size or by an increase in grain size.

4 DISCUSSION AND CONCLUSIONS

XRD, microprobe, backfield remagnetization of SIRM, *S*-ratios and hysteresis measurements all indicate that magnetite is the main magnetic mineral that is deposited at the atmosphere/bark interface and incorporated in outer 'A' bark samples. Due to the high number of different tree species and their distribution at the Milan site, a statistical analysis between the SIRM and magnetic susceptibility values found in the different species was not performed. The differences detected between different tree species and within the same species (see Fig. 8) are probably due to the tree location that is very sparse in the selected area. Thus, considering that all the tree species sampled in this study show similar tree bark patterns, the evaluation of the results obtained for the analysed parameters was based on their spatial distribution. The spatial distribution of susceptibility, SIRM and magnetite concentration shows a strong dependence on distance from roads with traffic and more importantly tram stops. This suggests that the main sources of magnetite in the Milan test

site are abrasion of tram braking systems and vehicle combustion processes. Outer 'A' bark samples from Area 1 closest to roads and tram stops have the highest susceptibility and SIRM, and therefore highest magnetite concentration. Outer 'A' bark samples from Area 2 have values that are comparable to the substantially pollution-free Santa Caterina control site.

Our results are in agreement with previous biomonitoring investigations conducted on tree leaves, which also identified magnetite as the main carrier of the magnetic signal (e.g. Moreno *et al.* 2003; Urbat *et al.* 2004; Mitchell & Maher 2009). They also are compatible with other studies, which identified trams and vehicles as the main sources of the magnetic particulate (e.g. Kardel *et al.* 2012). What is important to note from our results is that the susceptibility and SIRM values in inner 'B' samples are invariably very low (susceptibility being frequently diamagnetic) and close to the susceptibility and SIRM values measured at the Santa Caterina control site. This finding has important implications on how trees serve as sinks for PM. Airborne magnetite particles will be collected through deposition on the exposed outer 'A' bark of trees immediate to the PM source. This magnetite is then partially encapsulated into the inner bark ('B', 'C' and 'D' samples), probably as far in as the suber tissue, where it then undergoes reductive dissolution (Catinon *et al.* 2008; Zhang *et al.* 2008; Catinon *et al.* 2009). Electron microprobe analyses support this hypothesis, showing that at least some of the magnetic particles are not just deposited on the bark external surface but are well integrated in it. Some images show also a partial fragmentation of the magnetite minerals, suggesting that plant physiological processes may dissolve or disintegrate magnetite particles incorporated in the bark, as observed for other types of atmospheric particles (e.g. Freer-Smith *et al.* 2004; Novak *et al.* 2006).
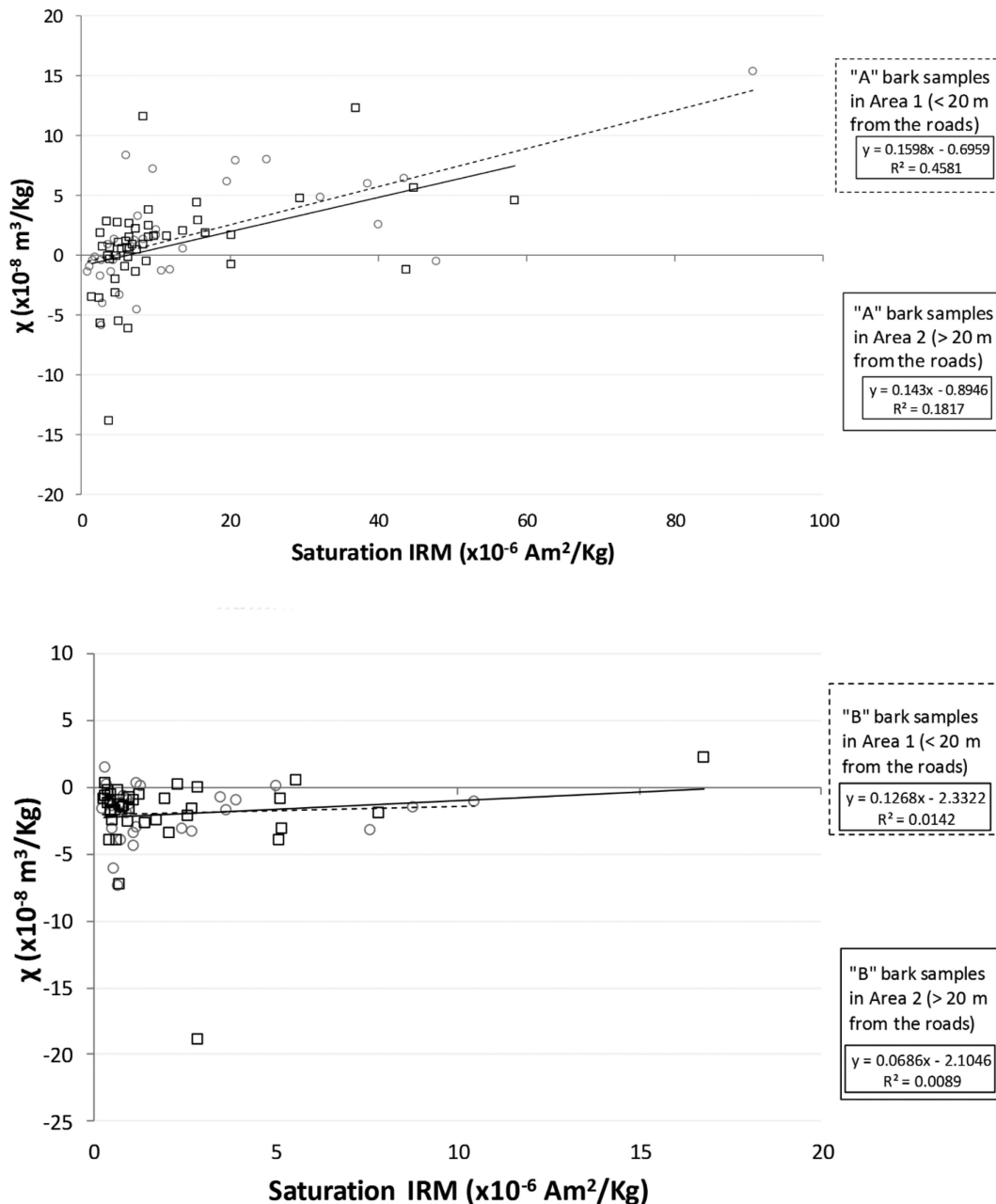
Figure 12. Plot of saturation IRM versus magnetic susceptibility values, calculated for (a) outer 'A' bark and (b) inner 'B' samples of trees sampled in Area 1 (discontinuous line) and in Area 2 (continuous line).

The implication that trees are capable of decomposing magnetite in their bark, emphasizes their role as pollution mitigating organisms. In this respect, this study is of interest for urban planning of green areas and infrastructures (e.g. Tong *et al.* 2016). Our results suggest that placing tree belts near roads with traffic and tram stops would help absorb airborne micrometric magnetite particles thus improving general air quality. Taking this idea further, it may be possible to design panels of synthetic, rugose bark that can be implemented either in lieu of—or together with—tree belts to improve trapping efficiency. Therefore, in conclusion, urban parks, tram stops and urban railways should always be enclosed in a dense network of tree belts and/or synthetic bark panels. In this way, even highly populated areas could still preserve oases with PM levels not

particularly higher than a mountain village, at least relative to the types and sources of PM described here.

Santa Caterina Valfurva was issued by the Stelvio National Park.

REFERENCES

Bigi, A. & Ghermandi, G., 2014. Long-term trend and variability of atmospheric PM_{10} concentration in the Po Valley, *Atmos. Chem. Phys.,* **14,** 4895–4907.

Birben, E., Sahiner, U.M., Sackesen, C., Erzurum, S. & Kalayci, O., 2012. Oxidative stress and antioxidant defense, *World Allergy Organ. J.,* **5,** 9–19.

Bohm, P., Wolterbeek, H., Verburg, T. & Muslek, L., 1998. The use of tree bark for environmental pollution monitoring in the Czech Republic, *Environ. Pollut.,* **102,** 243–250.

Catinon, M., Ayrault, S., Boudouma, O., Asta, J., Tissut, M. & Ravanel, P., 2009. The inclusion of atmospheric particles into the bark suber of ash trees, *Chemosphere,* **77,** 1313–1320.

Catinon, M., Ayrault, S., Daudin, L., Sevin, L., Asta, J., Tissut, M. & Ravanel, P., 2008. Atmospheric inorganic contaminants and their distribution inside stem tissues of *Fraxinus excelsior* L., *Atmos. Environ.,* **42,** 1223–1238.

Chiesa, M., Perrone, M.G., Cusumano, N., Ferrero, L., Sangiorgi, G., Bolzacchini, E., Lorenzoni, A. & Ballarin Denti, A., 2014. An environmental, economical and socio-political analysis of a variety of urban air-pollution reduction policies for primary PM10 and NO_x: the case study of the Province of Milan (Northern Italy), *Environ. Sci. Policy,* **44,** 39–50.

Del Ventisette, C., Casagli, N., Fortuny-Guasch, J. & Tarchi, D., 2012. Ruinon landslide (Valfurva, Italy) activity in relation to rainfall by means of GBInSAR monitoring, *Landslides,* **9,** 497–509.

Donaldson, K., 2003. The biological effects of coarse and fine particulate matter, *Occup. Environ. Med.,* **60,** 313–314.

Dunlop, D.J., 2002. Theory and application of the Day Plot (M_{rs}/M_s versus H_{cr}/H_c) 2. Application to data for rocks, sediments, and soils, *J. geophys. Res.,* **107**(B3), 2057, doi:10.1029/2001JB000487.

Evans, M.E. & Heller, F., 2003. *Environmental Magnetism: Principles and Applications of Enviromagnetics*, Academic Press.

Faustini, A. *et al.*, 2011. The relationship between ambient particulate matter and respiratory mortality: a multi-city study in Italy, *Eur. Respir. J.,* **38,** 538–547.

Flanders, P.J., 1994. Collection, measurement, and analysis of airborne magnetic particulates from pollution in the environment, *J. appl. Phys.,* **75,** 5931–5936.

Freer-Smith, P.H., El-Khatib, A.A. & Taylor, G., 2004. Capture of particulate pollution by trees: a comparison of species typical of semi-arid areas (*Ficus nitida* and *Eucalyptus globulus*) with European and North American species, *Water Air Soil Pollut.,* **155,** 173–187.

Gualtieri, M., Ovrevik, J., Mollerup, S., Asare, N., Longhin, E., Dahlman, H.J., Camatini, M. & Holme, J.A., 2011. Airborne urban particles (Milan winter-PM2.5) cause mitotic arrest and cell death: effects on DNA, mitochondria, AhR binding and spindle organization, *Mutat. Res.,* **713,** 18–31.

Guéguen, F., Stille, P., Lahd Geagea, M. & Boutin, R., 2012. Atmospheric pollution in an urban environment by tree bark biomonitoring—Part I: Trace element analysis, *Chemosphere,* **86,** 1013–1019.

Hanesch, M., Scholger, R. & Rey, D., 2003. Mapping dust distribution around an industrial site by measuring magnetic parameters of tree leaves, *Atmos. Environ.,* **37,** 5125–5133.

Hoffmann, V., Knab, M. & Appel, E., 1999. Magnetic susceptibility mapping of roadside pollution, *J. Geochem. Explor.,* **60,** 313–326.

Hunt, A., Jones, J. & Oldfield, F., 1984. Magnetic measurements and heavy metals in atmospheric particulates of anthropogenic origin, *Sci. Total Environ.,* **33,** 129–139.

Johnston, K., Ver Hoef, J.M., Krivoruchko, K. & Lucas, N., 2001. *Using ArcGIS Geostatistical Analyst*, Esri Press.

Kam, W., Cheung, K., Daher, N. & Sioutas, C., 2011. Particulate matter (PM) concentrations in underground and ground-level rail systems of the Los Angeles Metro, *Atmos. Environ.,* **45,** 1506–1516.

Kardel, F., Wuyts, K., Maher, B.A. & Samson, R., 2012. Intra-urban spatial variation of magnetic particles: monitoring via leaf saturation isothermal remanent magnetisation (SIRM), *Atmos. Environ.,* **55,** 111–120.

Kim, K.H., Kabir, E. & Kabir, S., 2015. A review on the human health impact of airborne particulate matter, *Environ. Int.,* **74,** 136–143.

Kletetschka, G., 2011. Magnetic measurements on maple and sequoia trees, in *The Earth's Magnetic Interior*, pp. 427–441, eds Petrovský, E., Ivers, D., Harinarayana, T. & Herrero-Bervera, E., IAGA Special Sopron Book Series 1, Springer Science + Business Media B.V., Dordrecht, Netherlands.

Kletetschka, G., Žila, V. & Wasilewski, P.J., 2003. Magnetic anomalies on the tree trunks, *Stud. Geophys. Geod.,* **47,** 371–379.

Lehndorff, E., Urbat, M. & Schwark, L., 2006. Accumulation histories of magnetic particles on pine needles as function of air quality, *Atmos. Environ.,* **40,** 7082–7096.

Maher, B.A., Moore, C. & Matzka, J., 2008. Spatial variation in vehicle-derived metal pollution identified by magnetic and elemental analysis of roadside tree leaves, *Atmos. Environ.,* **42,** 364–373.

Maher, B.A. *et al.*, 2016. Magnetic pollution nanoparticles in the human brain, *Proc. Natl. Acad. Sci. USA,* **113,** 10 797–10 781.

Marcazzan, G.M., Vaccaro, S., Valli, G. & Vecchi, R., 2001. Characterisation of PM10 and PM2.5 particulate matter in the ambient air of Milan (Italy), *Atmos. Environ.,* **35,** 4639–4650.

Masetti, M., Nghiem, S.V., Sorichetta, A., Stevenazzi, S., Fabbri, P., Pola, M., Filippini, M. & Brakenridge, G.R., 2015. Urbanization affects air and water in Italy's Po Plain, *EOS, Trans. Am. geophys. Un.,* **96,** 13–16.

Matzka, J & Maher, B.A., 1999. Magnetic biomonitoring of roadside tree leaves: identification of spatial and temporal variations in vehicle-derived particulates, *Atmos. Environ.,* **33,** 4565–4569.

McIntosh, G., Gómez-Paccard, M. & Osete, M.L., 2007. The magnetic properties of particles deposited on *Platanus x hispanica* leaves in Madrid, Spain, and their temporal and spatial variations, *Sci. Total Environ.,* **382,** 135–146.

Mitchell, R. & Maher, B.A., 2009. Evaluation and application of biomagnetic monitoring of traffic-derived particulate pollution, *Atmos. Environ.,* **43,** 2095–2103.

Moreno, E., Sagnotti, L., Dinarès-Turell, J., Winklers, A. & Cascella, A., 2003. Biomonitoring of traffic air pollution in Rome using magnetic properties of tree leaves, *Atmos. Environ.,* **37,** 2967–2977.

Novak, D.J., Crane, D.E. & Stevens, J.C., 2006. Air pollution removal by urban trees and shrubs in the United States, *Urban Forest. Urban Green.*, **4,** 115–123.

Ozgen, S., Ripamonti, G., Malandrini, A., Ragettli, M.S. & Lonati, G., 2016. Particle number and mass exposure concentrations by commuter transport modes in Milan, Italy, *AIMS Environ. Sci.,* **3,** 168–184.

Pacheco, A.M.G., Freitas, M.C., Barros, L.I.C. & Figuera, R., 2001. Investigating tree bark as an air-pollution biomonitor by means of neutron activation analysis, *J. Radioanal. Nucl. Chem.,* **249,** 327–331.

Pelfini, M., Leonelli, G., Trombino, L., Zerboni, A., Bollati, I., Merlini, A., Smiraglia, C. & Diolaiuti, G., 2014. New data on glacier fluctuation during the climatic transition at 4000 cal. year BP from a buried log in the Forni Glacier forefield (Italian Alps), *Rend. Lincei,* **25,** 427–437.

Sagnotti, L., Macrì, P., Egli, R. & Mondino, M., 2006. Magnetic properties of atmospheric particulate matter from automatic air sampler stations in Latium (Italy): toward a definition of magnetic fingerprints for natural and anthropogenic PM_{10} sources, *J. geophys. Res.,* **111,** doi:10.1029/2006JB004508.

Sawidis, T., Breuste, J., Mitrovic, M., Pavlovic, P. & Tsigaridas, K., 2011. Trees as bioindicator of heavy metal pollution in three European cities, *Environ. Pollut.,* **159,** 3560–3570.

Szönyi, M., Sagnotti, L. & Hirt, A.M., 2008. A refined biomonitoring study of airborne particulate matter pollution in Rome, with magnetic measurements on *Quercus Ilex* tree leaves, *Geophys. J. Int.,* **173,** 127–141.

Tong, Z., Baldauf, R.W., Isakov, V., Deshmukh, P. & Zhang, K.M., 2016. Roadside vegetation barrier designs to mitigate near-road air pollution impacts, *Sci. Total Environ.,* **541,** 920–927.

Urbat, M., Lehndorff, E. & Schwark, L., 2004. Biomonitoring of air quality in Cologne conurbation using pine needles as passive sampler. Part I: Magnetic properties, *Atmos. Environ.,* **38,** 3781–3792.

Vecchi, R. *et al.*, 2008. A mass closure and PMF source apportionment study on the sub-micron sized aerosol fraction at urban sites in Italy, *Atmos. Environ.,* **42,** 2240–2253.

Zhang, C., Huang, B., Piper, J.D.A. & Luo, R., 2008. Biomonitoring of atmospheric particulate matter using magnetic properties of *Salix matsudana* tree ring cores, *Sci. Total Environ.,* **393,** 177–190.

Zhou, Y.M., Zhong, C.Y., Kennedy, I.M. & Pinkerton, K.E., 2003. Pulmonary response of acute exposure to ultrafine iron particles in healthy adult rats, *Environ. Toxicol.,* **18,** 227–235.